Synthesis of rutile titania powders: Agglomeration, dissolution, and reprecipitation phenomena

Sascha M. Klein and Joon Hwan Choi
Materials Department, University of California at Santa Barbara, Santa Barbara, California 93106
David J. Pine
Chemical Engineering Department, University of California at Santa Barbara, Santa Barbara, California 93106
Fred F. Lange
Materials Department, University of California at Santa Barbara, Santa Barbara, California 93106

(Received 10 September 2002; accepted 25 March 2003)

Rutile titania powders were synthesized via a sol-gel/hydrothermal process using nitric acid as the catalyst. A molar acid to alkoxide ratio of 10 and a water to alkoxide molar ratio of 250 produced 100% rutile powders when precipitated below 45 °C. Higher temperatures yielded initially either anatase or mixtures of anatase and rutile. Spherulitic growth produced cauliflower-shaped agglomerates with a mean size of 760 nm. The agglomerates could be broken apart into approximately 100-nm large broomlike agglomerates via a dissolution and reprecipitation process when reacted with approximately 2.4 molar nitric acid. Transmission electron microscopy observations showed that the broomlike agglomerate consisted of linear clusters of rodlike agglomerates composed of crystallographically aligned, primary particles approximately 4 nm in size.

I. INTRODUCTION

Titania (TiO_2) has three polymorphs: anatase, brookite, and rutile. All are constructed with Ti–O_6 octahedra and differ only in their octahedral linkage. In anatase, four of twelve octahedral edges are shared with neighboring octahedral; in brookite three and in rutile two octahedral share edges.[1] Although rutile is the thermodynamically stable form of titania, generally anatase, and occasionally brookite, crystallizes first during synthesis. Anatase starts to transform to rutile at >600 °C.[2] The different crystalline structures of titania have different material properties including density, index of refraction, and catalytic properties.

Titania, a wide band gap semiconductor, can be used in a variety of applications including gas sensors,[3] catalysts,[4] photovoltaic solar cells,[5] and pigments.[6] Recently, titania also gained interest as a material used in photonic band gap crystals for the visible spectrum of light due to its high index of refraction ($n_{rutile} \approx 2.9$)[7] and low absorption.[8–10]

Industrially, titania is produced by the sulfate and chloride processes.[11] Other synthesis methods include inert gas condensation,[12] oxidation-hydrothermal synthesis of metallic Ti,[13] and hydrothermal methods.[14–16]

Most applications for titania require specific material properties and therefore, a specific crystalline structure. Depending on the synthesis recipe, the crystalline structure of anatase,[17] rutile,[18] or brookite,[19] as well as mixtures of the three can be synthesized by the hydrothermal method.

The rutile structure can be obtained by heating the other polymorphs to high temperatures >600 °C to cause a phase change.[2] Generally, the initial synthesis method of titania determines the approximate phase-transformation temperature.[20] Other variables that also influence the transformation temperature are the synthesis atmosphere[21] and pressure,[2] as well as grain size[22,23] and packing density of the powder compact.[24] Also, doping TiO_2 with a second phase prior to crystallization[15] and mechanical activation by attrition milling of the crystalline powders[25,26] aid in lowering the transformation temperature. In the case of hydrothermal synthesis, titania with the rutile structure can be stabilized either by the addition of a SnO_2[27] or with the help of a catalyst such as nitric,[28] hydrochloric,[29] or citric acid.[30]

The exact catalytic mechanism explaining the formation of the rutile structure at temperatures as low as room temperature is not fully understood. Cheng and coworkers[15] suggested a mechanism based on their work using $TiCl_4$ as the titania precursor. After hydrolysis of the precursor, a Ti(IV) complex is assumed to be present with the formula $[Ti(OH)_nCl_m]^{2-}$, with $m + n = 6$ (due to the octahedral coordination of Ti). High acidity leads to a smaller number of OH^- groups (small n), while low

acidic concentrations will produce less Cl^- and therefore a smaller value for m. The linkage between $Ti–O_6$ octahedrons is carried out by a dehydration reaction between the OH ligands of adjacent $[Ti(OH)_nCl_m]^{2-}$ complex ions. As mentioned above, edge-shared bonding favors the anatase structure, while corner-shared bonding preferably leads to rutile. To form an edge-shared bond, two dehydration reactions between a pair of $[Ti(OH)_nCl_m]^{2-}$ must occur simultaneously, which is less likely at high acidic concentrations. Thus, high acidic concentrations appear preferable for synthesizing rutile.

In the current work, we detail a hydrothermal synthesis method that produces pure rutile titania using nitric and hydrochloric acid as the catalysts. We describe how agglomerates are formed, as well as their break up into smaller agglomerates during an acid treatment.

II. EXPERIMENTAL

Unless otherwise noted all chemicals were used "as received" without further purification. The titanium alkoxide precursors were purchased from Gelest (Gelest Inc., PA) and diluted as noted with the corresponding anhydrous alcohol (Aldrich, Milwaukee, WI). Either nitric or hydrochloric acid (Fisher Scientific, Pittsburgh, PA) was used as the peptizing agent.

Synthesis formulations are described by the molar ratios of acid to titania precursor ($[H^+]/[Ti]$), the molar ratio of ethanol to alkoxide ([EtOH]/[Ti), and the molar ratio of water to alkoxide ($[H_2O]/[Ti]$), denoted as R, which was fixed at 250; [EtOH]/[Ti] was set to 10. If not otherwise noted, the $[H^+]/[Ti]$ ratio was adjusted to 10. Due to the water reactivity of the precursor, the chemicals were stored in a N_2 glove box. Initially, the alkoxides were diluted in alcohol and placed into a syringe inside the N_2 glove box. Outside the glove box, the alkoxide/alcohol mixture was added dropwise to a stirred, water bath. White flocks were produced as soon as the alkoxides came into contact with the water bath indicating that the titania precursor immediately hydrolyzed. After stirring the reaction for 2 h, the precipitates were filtered and washed with deionized water five times to remove the alcohol[31] and any unreacted species dissolved in the water/alcohol phase. The filtered titanium hydroxide cake was then placed into an acidic solution and stirred mechanically. Within a few minutes the white precipitates dissolved (peptized) to produce a clear, slightly bluish and transparent solution. If not otherwise noted, the peptized solution was stirred for 24 h prior to heating. To reaggregate (reprecipitate) the titania powder, the peptized solution was heat treated between room temperature and 85 °C for different periods. For heat treatments up to 85 °C, the acidic titania solution was placed into a three-neck flask that sat in a heated silicon oil bath. One neck was equipped with a water-cooled condenser to avoid evaporation of solution, while the two remaining necks were closed with glass stoppers to allow samples to be removed. During the synthesis, the solution was stirred with a magnetic stir bar. After complete precipitation of the TiO_2 powder, the sample was kept in the three-neck flask for further heat treatments below 100 °C.

During the study, it was discovered that cauliflower-shaped agglomerates were produced and these agglomerates could be broken apart by further acid treatment, which was more effective at temperatures above 100 °C. For heat treatments above 100 °C, the solutions were placed into a Teflon-lined acid digestion bomb (Parr Instrument Company, IL) for hydrothermal treatments between 100 and 250 °C. Unless otherwise noted, the Teflon liner was filled to two thirds of its total volume (45 ml).

Except for particle-size measurements, samples were taken from the reaction vessel, cooled, washed via centrifugation and filtration with deionized water, and dried at 60 °C. Washing and drying caused the particles to agglomerate. The powder sample's weight was determined with the help of a balance after washing and drying the powders.

The particle-size distribution of the titania powders was determined by static light scattering with a Malvern Master Sizer 2000 (Malvern Instruments Inc., MA). A slurry sample (approximately 1 ml) was taken directly from the reaction vessel and directly inserted into the water pump attached to the particle-size analyzer.

The crystalline phase of titania was determined by x-ray diffraction (XRD) analysis (Philips Expert, Philips Inc., Eindhoven, The Netherlands). The phase compositions of the titania samples were obtained from the equation suggested by Spurr and Myers:[32]

$$x_A = \frac{1}{1 + 1.26 \times \frac{I_R}{I_A}} \quad ,$$

where x_A is the weight fraction of anatase in the mixture and I_A and I_R are the XRD intensities of anatase and rutile. For the calculations here the (101) anatase and the (110) rutile peaks were chosen.

Scanning electron microscopy (SEM) images were carried out either with a Joel 6300F or a Joel 6340F. The transmission electron microscopy (TEM) images were taken with a Joel 2000 FX.

III. RESULTS

No significant difference could be observed for the three titania precursors, titanium-ethoxide, -isopropoxide, and -butoxide. Also, no difference was observed

when either hydrochloric or nitric acid was chosen as the catalyst. Therefore the results reported below are only for synthesis with titanium (IV)-ethoxide and nitric acid.

A $[H^+]/[Ti]$ ratio of 10 was found to synthesize titania with a very large rutile to anatase ratio. Lower ratios (0.1, 1) increased the anatase content, while much higher $[H^+]/[Ti]$ ratios (40 to 160) did not allow precipitation of titania.

With a $[H^+]/[Ti]$ ratio of 10 and R = 250, it was found that the reaggregation temperature had a significant influence on the crystalline phase of the synthesized powders. Figure 1 shows the ratio of rutile to anatase versus synthesis time for different temperatures. A hydrothermal reaggregation temperature of 65 and 85 °C initially produced a mixture of anatase and rutile. During the heat treatment at either 65 or 85 °C, all anatase dissolved and precipitated as 100% rutile. Treatments at 45 and 25 °C produced pure rutile from the beginning. Figure 2 reports the XRD data for 2Θ between 20° and 30° for solutions treated at 65 °C for various periods. The (101) anatase peak decreased with reaction time until only the (110) rutile peak was present.

Figure 3 reports the amount of rutile powder precipitated with time. The 45 °C sample fully precipitated the titania in solution after approximately three days, while even after 27 days, the sample treated at 25 °C did not precipitate all of its titania. In the following the results were obtained with titania powders that were synthesized for three days at 45 °C. Subsequent heat treatments were either performed at temperatures below 100 °C in a three-neck flask, as described above, or transferred to a hydrothermal bomb for treatments above 100 °C.

Figure 4 reports the particle-size distribution for titania fully synthesized at 45 °C and then further treated at the same temperature for prolonged periods. The powder synthesized for two days has a broad, unimodal size distribution with a D_{50} value (50% of all powder particles had a particle size equal or smaller than this value) of approximately 760 nm. After five days of further treatment, a second peak developed centered around particle sizes of 100 nm while the peak at 760 nm diminished. Longer reaction periods led to smaller particles while the amount of larger particles decreased until only small particles around 100 nm were present. A sample with a D_{50} value of 97 nm was obtained after about 90 days. These data show that a prolonged acid treatment of fully synthesized titania led to smaller particles.

Figure 5 shows a SEM image of dried rutile titania powders produced after two to five days at 45 °C for the conditions discussed in the last paragraph. Individual spherical agglomerates, each with a size of approximately 1 μm are visible. The particles are cauliflower-shaped, with fine needles protruding from the surface.

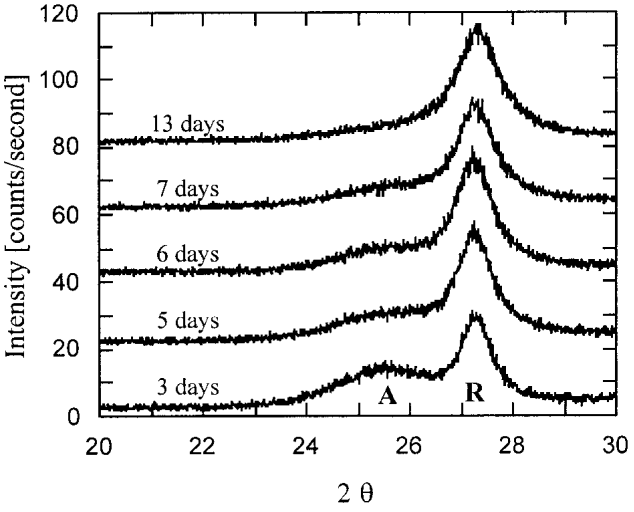

FIG. 2. XRD scans for a sample reaggregated at 65 °C.

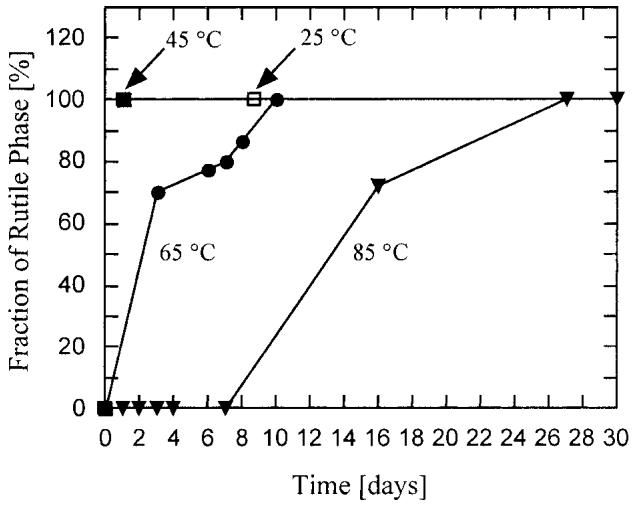

FIG. 1. Phase composition of titania powder samples synthesized at 25, 45, 65, and 85 °C during periods of up to 30 days.

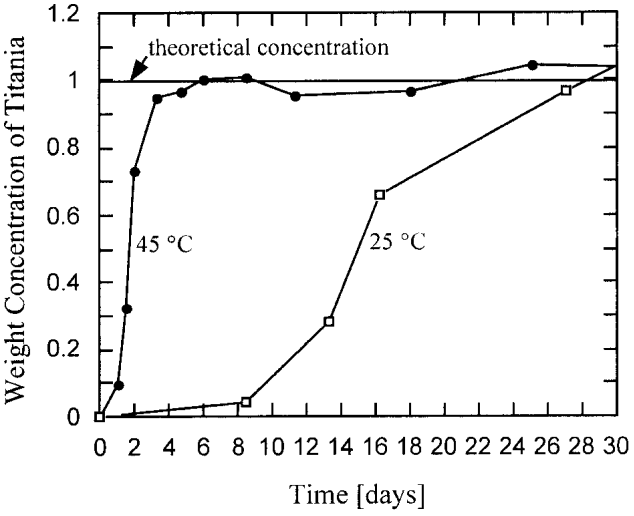

FIG. 3. Weight concentration of rutile powders synthesized at 25 and 45 °C as a function of synthesis period.

The morphology of a rutile powder sample possessing a bimodal size distribution is shown in Fig. 6. For these prolonged treatments, many of the larger cauliflower-shaped agglomerates have broken apart revealing their interior [Fig. 6(a)]. In Fig. 6(b) an image of a much smaller, individual agglomerate that broke away from the spherical agglomerate is shown. After comparison with the particle in Fig. 6(a), it can be observed that the larger spherical particles are composed of many of these smaller agglomerates as depicted in Fig. 6(b).

A SEM image of the titania powders after about 90 days of heat treatment is shown in Fig. 7. Nano-sized broomlike agglomerate, composed of linear particles were observed. Figure 8 shows TEM dark-field and bright-field images of such a broomlike agglomerate. It shows that the particles are composed of rodlike particles that are themselves composed of very small, primary particles, linearly attached to one another. The images show the oriented attachment of crystallites forming the linear, rodlike particles; this crystallographic alignment is also confirmed by the inserted diffraction pattern in Fig. 8(b).

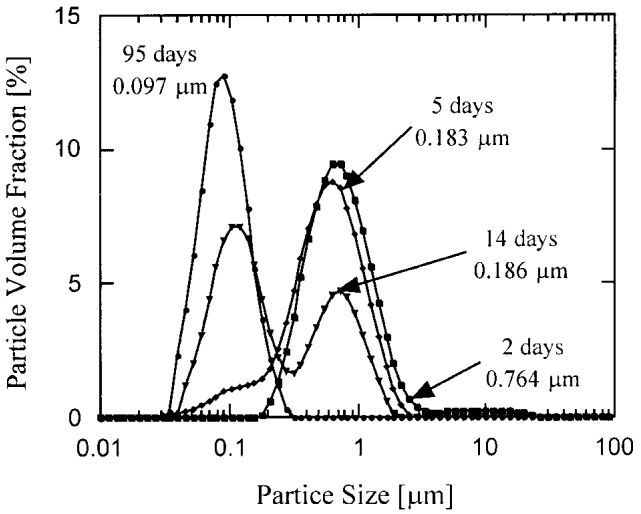

FIG. 4. Particle-size distribution for rutile titania powders re-aggregated at 45 °C.

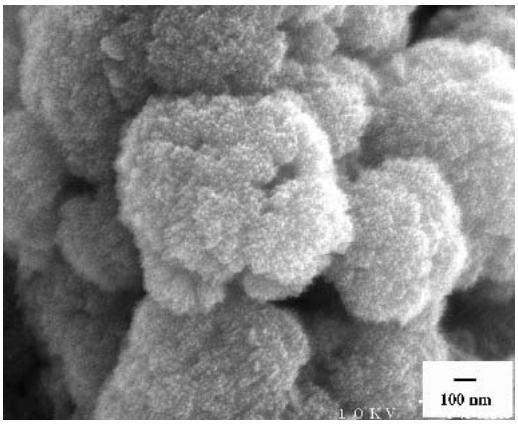

FIG. 5. Cauliflower-shaped, spherical agglomerates of rutile powders are present during the early synthesis stage.

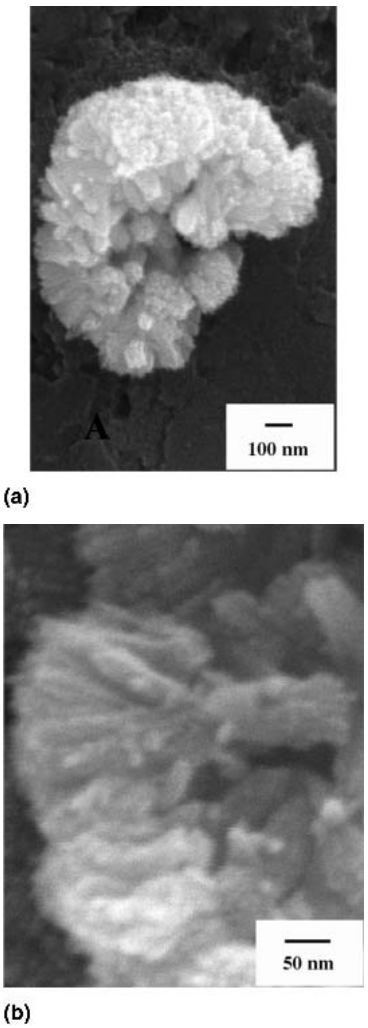

FIG. 6. (a) Spherical agglomerate after some breakup occurred. (b) Internal structure reveals that the spherical particle is composed of broomlike units.

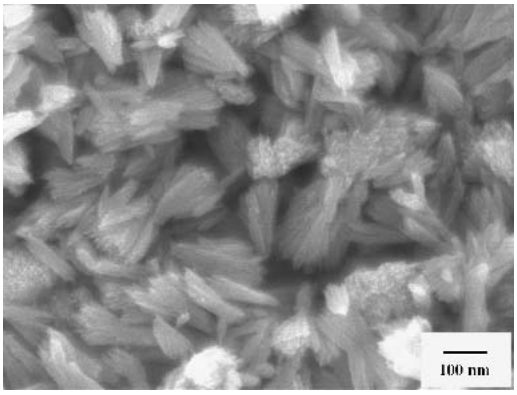

FIG. 7. Small broomlike particles are visible after about 90 days of hydrothermal treatment at 45 °C.

Powders heat treated at higher temperatures broke up quicker than those at lower temperatures. Figure 9 shows the relationship between the particles' D_{50}-values versus reaction time for samples treated at 25 and 45 °C. After about 20 days, most of the 45 °C sample had broken into 100 nm units, while the sample at room temperature needed about 60 days to develop a similar D_{50}-value. However, the final particle size was independent of the reaction temperature for the period investigated. Samples heat treated below 100 °C were generally stirred with the help of a magnetic stir bar. Stirring helped break up the initial, cauliflower-shaped agglomerates more rapidly, but the final particle size was independent of stirring.

To investigate the influence of higher temperatures, titania powders were first synthesized at 45 °C for three days to obtain the rutile crystalline structure and then placed into acid digestion bombs and heated to higher temperatures under the same acidic conditions. Hydrothermal heat treatments were performed at 150 °C for a period of 1 to 24 h. Figure 10 shows the change in particle-size distribution with reaction period. The starting powders possessed a very broad size distribution. After hydrothermally treating the sample for 2 h most of the large particles were already broken up into small, nano-sized particles. A reaction period of 8 h was enough to break apart the particles into powders with a D_{50}-value of 90 nm. The resulting particle morphology is shown in Fig. 11(a). The initial spherical, cauliflower-shaped agglomerates broke up into nano-sized, blocklike particles. Figure 11(b) depicts an earlier stage during the break-up process. An agglomerate is shown that consists of only very few particles, while most other particles have been converted into large, rutile particles. As shown in Fig. 12, TEM observations revealed each particle to be a single crystal.

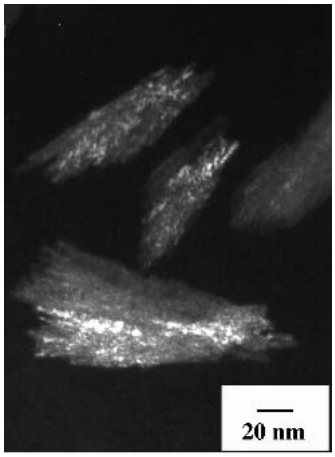

(a)

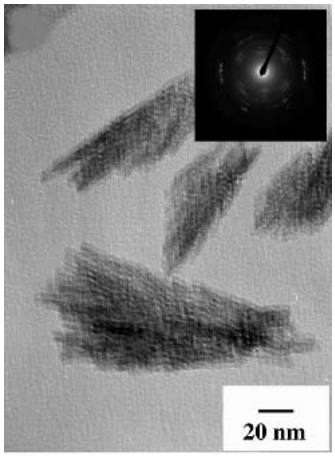

(b)

FIG. 8. TEM (a) dark-field and (b) bright-field images of broomlike agglomerates. Images and the diffraction pattern reveal that individual linear, needlelike particles are composed of linearly attached crystallites.

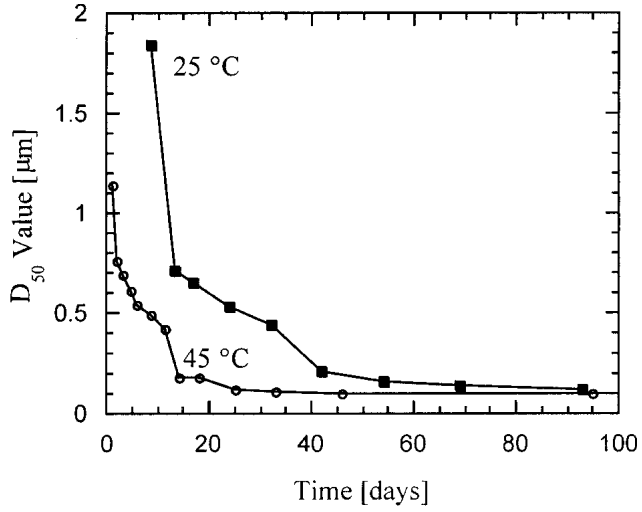

FIG. 9. D_{50} value as a function of reaction period for samples treated at 25 and 45 °C.

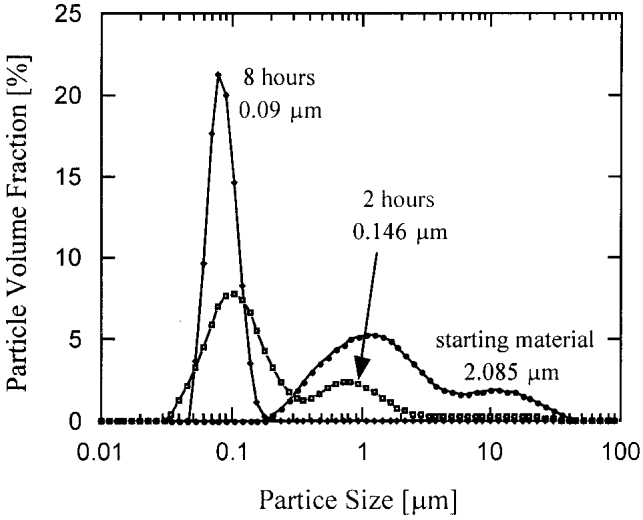

FIG. 10. Particle size distribution for powders hydrothermally treated at 150 °C for 2 to 8 h.

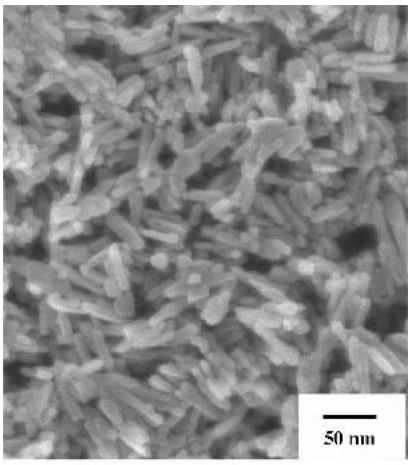

(a)

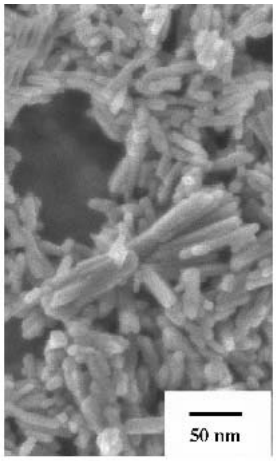

(b)

FIG. 11. (a) Rodlike morphology of particles hydrothermally treated at 150 °C for 8 h. (b) A larger agglomerate is shown displaying an earlier stage during the particle breakup.

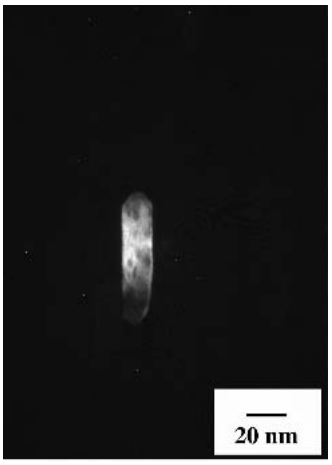

(a)

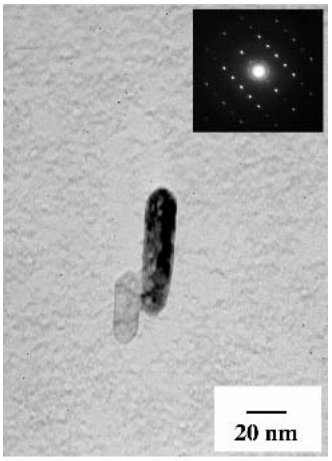

(b)

FIG. 12. TEM (a) dark-field and (b) bright-field images of hydrothermally treated powder particles. The diffraction pattern reveals particles to be rutile single crystals.

IV. DISCUSSION

The hydrothermal method presented here allows the direct synthesis of titania powders with the rutile structure. It was evident that high acidity was important for synthesizing rutile. This observation is consistent with the idea of Cheng *et al.*[15] who suggested that a large number of Cl^- (or NO_3^-) ions would produce octahedrally coordinated complexes $[Ti(OH)_nCl_m]^{2-}$ with $m > n$ to favor corner shared bonding between the complexed ions and thus, the crystallization of rutile instead of anatase, which is promoted with edge shared bonding.

In addition to the need for a highly acidic condition, the synthesis temperature played an important role. Solutions heated to temperatures $\geqslant$65 °C initially synthesized anatase, which dissolved and later grew as rutile agglomerates. Apparently, higher temperatures favor edge bonding of the octahedrally coordinated Ti complexes, and the greater rate of nucleation of anatase. However, although fewer in number, rutile nuclei are certainly favored during growth due to their apparent lower free energy. That is, under any condition explored in this work, it appears that the faster precipitating anatase will eventually dissolve to produce titania with the rutile structure.

Solution reprecipitation played a strong role in the formation of the observed cauliflower-shaped agglomerates. Such agglomerates are formed by a spherulitic growth mechanism known to occur also in other inorganic materials synthesized from a solution. For example, Busch *et al.*[33] observed spherulitic growth of fluorapatite in gelatin matrices by biomimetic growth and Qi[34] observed the same for $BaSO_4$ particles. The resulting particle morphology observed here for rutile titania is identical to the observation made by Busch *et al.* and Qi *et al.*

The spherulitic growth phenomenon occurs by the addition of nanoparticles to the ends of growing rods, which are themselves composed of nanoparticles. It

appears that the particles are attracted to one another because of the very high concentration of counter-ions in the very acidic solution (i.e., a condition that produces attractive interparticle potentials). Very small deviations in growth direction cause the "rods" to spread apart and eventually grow around themselves to form two "cauliflowers" joined at their base. Since material is being synthesized throughout this process, once a particle touches the end of a rod, or adjacent rods touch one another, the particles will sinter to the rod; likewise, the rods will sinter to one another. That is, the locations where the particle touches the rod, or the rods touch one another are locations of high free energy (high surface to volume ratio). Material added to these locations cause necks to grow between the touching particles/rods. In fact, neck growth (sintering) is favored over particle growth because neck growth decreases the surface to volume ratio much faster than particle growth. Thus, the cauliflower-shaped agglomerates are not only a collection of touching particles but a collection of sintered particles.

The reason the collection of touching, sintered particles produce the cauliflower-shaped agglomerate instead of a very open agglomerate with fractal dimension (for example, by diffusion-limited aggregation) is not known in detail. Busch *et al.*[33] postulated that the spherulitic growth of the apatite agglomerates was because the primary apatite particles are piezoelectric and thus have a polar moment; they will attract one another end to end. Neither anatase nor rutile have a polar moment. However, Penn and Banfield[17] have shown with high-resolution studies that anatase nano-particles, formed at pH = 3 form linear, rodlike agglomerates and the particle in these rods are crystallographically aligned relative to one another. Although effort in the current work was not successful in isolating single rod-shaped agglomerates (the high acidity of the synthesis solution caused irreversible changes in the particles when the acidity was reduced for TEM preparation), the particles in the rod-shaped arrangement of sintered particles in the broomlike agglomerates shown in Fig. 8 (TEM micrograph) are crystallographically aligned in the same manner reported by Penn and Banfield.[17] It can only be speculated that the planar surfaces that define the surface morphology of the rutile (or anatase) crystallites kinematically and/or energetically aligned themselves when adjacent particles form linear agglomerates.

The nitric acid not only acts as a catalyst for the rutile synthesis, but also, after the titania in solution was depleted, it could dissolve the titania to cause the cauliflower-shaped agglomerates to break apart at lower temperatures and coarsen at higher temperatures, via a dissolution-reprecipitation phenomenon. A similar deagglomeration phenomenon was observed for silicon nitride powders dispersed in water at pH = 9 by Laarz *et al.*[35] In their work, Laarz and Bergström showed that Si_3N_4 particles were bonded together with SiO_2, to form 50–200-μm agglomerates. Treatment in a very basic aqueous solution that promoted the dissolution of SiO_2 caused the larger agglomerates to break into smaller agglomerates with sizes of about 1 μm. They showed that the break-up process increased with increased temperature and increased pH value[12] that promoted the increased solubility of SiO_2 in water. Mild agitation also favored the break-up process of the Si_3N_4 agglomerates. In the current work, the nitric acid dissolves the titania causing the initially cauliflower-shaped agglomerates to break up into smaller broomlike agglomerates. It was also observed that the break-up process could be sped up with the help of a magnetic stir bar at temperatures of 25 °C, but even without stirring the particles separated into the same size particles. When powder was synthesized at low temperatures and then hydrothermally treated at 150 °C, the particles grew by a solution-reprecipitation (Ostwald ripening) mechanism into single-crystalline particles with an average size about 100 nm.

V. CONCLUSION

Titania crystallized in the rutile structure could be synthesized by a hydrothermal method under highly acidic conditions. The important variables in the synthesis were found to be the $[H^+]/[Ti]$ molar ratio, the synthesis temperature, and the synthesis period. HNO_3 was used as the peptizing agent, acting as the catalyst to stabilize the rutile phase, and produced cauliflower-shaped agglomerates. After the Ti-precursor was depleted, the HNO_3 then acted as a dissolution agent to help break apart the larger agglomerates into smaller, 100 nm units. Single-crystalline rutile particles about 100 nm in size could be produced by coarsening the particles in a hydrothermal bomb at 150 °C.

ACKNOWLEDGMENT

This work was supported by the MRL Program of the National Science Foundation under Award No. DMR00-80034.

REFERENCES

1. H.W. Jaffe, *Crystal Chemistry and Refractivity* (Dover Publications, 1996).
2. F.A. Hummel, *Introduction to Phase Equilibria in Ceramic Systems* (Marcel Dekker, 1984).
3. M. Ferroni, V. Guidi, and G. Martinelli, Nano-Struct. Mater. **7,** 709 (1996).
4. Z. Ma, Y.Yue, X. Deng, and Z. Gao, J. Molecular Catal. A: Chem. **178,** 97 (2002).

5. U. Bach, D. Lupo, P. Comte, J.E. Moser, F. Weissoertel, J. Salbeck, H. Spreitzer, and M. Grätzel, Nature **395,** 583 (1998).
6. W.P. Hsu, R. Yu, and E. Matijevic, Dyes Pigments **19,** 179 (1992).
7. G.R. Fowles, *Introduction to Modern Optics* (Dover Publications, New York, 1975).
8. R. Biswas, M.M. Sigalas, G. Subramania, and K-M. Ho, Phys. Rev. B **57,** 3701 (1998).
9. V.N. Manoharan, A. Imhof, J.D. Thorne, and D.J. Pine, Adv. Mater. **13,** 447 (2001).
10. G. Subramanian, V.N. Manoharan, J.D. Thorne, and D.J. Pine, Adv. Mater. **11,** 1261 (1999).
11. N.N. Greenwood and E. Earnshaw, *Chemistry of the Elements* (Pergamon Press, 1984).
12. R.W. Siegel, S. Ramasamy, H. Hahn, L. Zongquan, and L. Ting, J. Mater. Res. **3,** 1367 (1996).
13. Q. Chen, Y. Qian, Z. Chen, G. Zhou, and Y. Zhang, Mater. Lett. **22,** 77 (1995).
14. C.J. Brinker and G.W. Scherer, *Sol-Gel Science* (Academic Press, 1990).
15. H. Cheng, J. Ma, Z. Zhao, and L. Qi, Chem. Mater. **7,** 663 (1995).
16. W.W. So, S.B. Park, K.J. Kime, and S.J. Moon, J. Colloid Interface Sci. **191,** 398 (1997).
17. R.L. Penn and J.F. Banfield, Geochim. Cosmochim. Acta. **63,** 1549 (1999).
18. W.W. So, S.B. Park, and S.J. Moon, J. Mater. Sci. Lett. **17,** 1219 (1998).
19. I. Keesmann, Z Anorg. Allg. Chem. **346,** 30 (1966).
20. A.F. Holleman and E. Wiberg, *Lehrbuch der Anorganischen Chemie* (Walter de Gruyter, 1985).
21. J.A. Gamboa and D.M. Pasquevich, J. Am. Ceram. Soc. **75,** 2934 (1992).
22. H. Zhang and J.F. Banfield, J. Mater. Chem. **8,** 2073 (1998).
23. X-Y. Ding, X-H. Liu, and Y-Z. He, J. Mater. Sci. Lett. **15,** 1789 (1996).
24. J-P. Ahn, J-K. Park, and G. Kim, Nano-Struct. Mater. **10,** 1087 (1998).
25. E.M. Kostic, S.J. Kiss, S.B. Boskovic, and S.P. Zec, Am. Ceram. Soc. Bull. **76,** 60 (1997).
26. S. Sen, M.L. Ram, S. Roy, and B.K. Sarkar, J. Mater. Res. **14,** 841 (1999).
27. Y. Suwa, Y. Kato, S. Hirano, and S. Naka, J. Soc. Mater. Japan **31,** 955 (1982).
28. R.R. Bacsa and M. Grätzel, J. Am. Ceram. Soc. **79,** 2185 (1996).
29. K. Nomura, Y. Takasuka, and S. Hirano, Third Euro-Ceram. **1,** 381 (1993).
30. H. Yin, Y. Wada, T. Kitamura, S. Kambe, S. Murasawa, H. Mori, T. Sakata, and S. Yangida, J. Mater. Chem. **11,** 1694 (2001).
31. D.C. Hague and M.J. Mayo, J. Am. Ceram. Soc. **77,** 1957 (1994).
32. R.A. Spurr and H. Myers, Anal. Chem. **29,** 760 (1957).
33. S. Busch, H. Dolhaine, A. DuChesne, S. Heinz, O. Hochrein, F. Laeri, O. Podebrand, U. Vietze, T. Weiland, and R. Kniep, Eur. J. Inorg. Chem. 1643 (1999).
34. L. Qi, H. Cölfen, and M. Antonietti, Chem. Mater. **12,** 2392 (2000).
35. E. Laarz, B.V. Zhmud, and L. Bergström, J. Am. Ceram. Soc. **83,** 2394 (2000).